J Cutan Pathol 1994: 7–15
Printed in Denmark – all rights reserved

Journal of
Cutaneous Pathology
ISSN 0303-6987

Differentiation between malignant melanomas and benign melanocytic nevi by computerized DNA cytometry of imprint specimens*

Wilhelm Stolz[1], Thomas Vogt[1], Michael Landthaler[1], Siegfried Hempfer[2], Paul Bingler[2] and Wolfgang Abmayr[3]

[1]Department of Dermatology, University of Regensburg, [2]Department of Dermatology, University of Munich, [3]Department of Informatics and Mathematics, Fachhochschule München, Munich, Germany

Recently image analysis (IA) and DNA-cytophotometry (CP) have proved to be useful for the differentiation between benign and malignant melanocytic lesions on paraffin sections. Since, on sections, these procedures are very time-consuming, we tested in the present study whether IA of imprint specimens, which can be evaluated in less than 30 minutes, might also be sufficient. In 39 malignant melanomas (MM), 18 melanocytic nevi (MN), and 6 dysplastic nevi (DN), 12 different morphometric and DNA cytometric features were determined in 100 randomly selected nuclei. In univariate analysis, 5 features were found to be significantly different between the benign and malignant groups ($p<0.0001$): mean value (MAREA) and standard deviation (SAREA) of nuclear area and the 80th, 90th, and 95th percentiles of DNA distribution. Using SAREA, the best univariate feature, 82.5% of the cases could be correctly separated. In multivariate analysis with a combination of three features – standard deviation of nuclear area (SAREA), mean DNA value (MDNA), and 95th percentile of DNA distribution (PERC95) – a correct diagnosis was achieved in 89.5% of the cases. Results obtained in the cases of DN indicated an increased proliferation, but did not allow the separation of DN from MM and MN. Since our technique allows a rapid analysis without loss of tissue, which might be important for histological analysis, and the classification rates are equal or still higher than reported in studies on sections, imprints of melanocytic lesions seem to be most appropriate for the calculation of DNA cytometric features as helpful diagnostic criteria in equivocal melanocytic lesions.

Stolz W, Vogt T, Landthaler M, Hempfer S, Bingler P, Abmayr W. Differentiation between malignant melanoma and benign melanocytic nevi by computerized DNA cytometry of imprint specimens*. J Cutan Pathol 1994: 21: 7–15. © Munksgaard 1994.

Wilhelm Stolz, MD, Department of Dermatology, University of Regensburg, Franz-Josef-Strauss-Allee 11, D 93042 Regensburg, Germany

Accepted for publication July 9, 1993

*Supported by the Deutsche Forschungsgemeinschaft (Grant Sto 189/1–1 and 189/1–2).
This paper is a major part of an MD thesis at the University of Munich (55).

The histologic differential diagnosis between primary malignant melanoma (MM) and benign melanocytic nevi (MN) can be difficult, which might be due to the lack of generally accepted and adequate reproducible criteria (1–3) as shown especially in the survey of Jones (1). In that study, experts in dermatopathology were asked to delineate their five most important criteria for diagnosis of MM (1). Fifty distinct criteria were mentioned by 48 histopathologists, demonstrating considerable heterogeneity and controversy. Cytologic atypia was the most frequently mentioned criterion. However, also cytologic atypia is not clearly defined and can be related to cellular size, nuclear size and shape, as well as to nucleolar morphology. Also in an international pathologists congruence survey, an overall consistency in determining histological features in MM of only 70% was reported (4). Despite this discrepancy, in the majority of the cases the diagnosis rendered by a dermatopathologist based on years of accumulated experience is highly reliable.

To obtain more precise and objective diagnostic criteria, several laboratory techniques have been applied, e.g. morphometry (5–7), monoclonal antibody labeling (8–10), cell culture studies (11), chromosome analysis (12–14) and, due to the significance of DNA for diagnosis of various human neoplasms (15), DNA measurements (16 – 21). The latter can be performed by flow cytometry (FC) (22), cytophotometry (CP) (23), or by image analysis (IA) systems (24). The diagnostic efficiency of FC strongly varied in the studies performed for discrimination between MM and MN from 52.8% to 100% with a mean value of 74.5% (25–30). This discrepancy might be due to the difficulty in FC to recognize a small number of aneuploid cells among background activity. Also autofluorescence of melanocytes and stroma cells may disturb data analysis as indicated by Newton et al. (31). In contrast to FC, efficiency of IA and CP for discrimination of MM and MN was found to be higher (16, 17, 29, 32–35), ranging from 76.1% to 100% with a mean value of 87.5%. However, DNA measurements on sections are more time-consuming because, at least in a part of the nuclei, the exact border has to be determined interactively for each cell. In addition, frequently entire nuclei are not completely located within the section, thus leading to problems in data analysis. These difficulties can be avoided by using imprint specimens for DNA measurements. This offers three main advantages: a) Due to the high contrast between the nuclei and the background, automatic and therefore rapid segmentation of the nuclear border is possible, leading to a significant decrease of analysis time. b) Bias due to measurements of sectioned nuclei can be avoided. c) An immediate preparation after excision of a suspicious lesion is possible also without loss of tissue, which may be required for subsequent histologic, immunohistologic, and molecular biologic analyses.

Table 1. Diagnoses and patients' characteristics of the 63 cases studied

Diagnosis	Number of cases	Age (mean) (years)	Female/ male
melanocytic nevi	18	26.6	12/6
dysplastic nevi	6	55.2	2/4
SSM	19	52.9	11/8
NMM	14	51.6	5/9
unclassified MM	1	61.0	0/1
metastases	5	60.	4/1

In our hands, imprint specimens proved to be also very useful in diagnostic and prognostic evaluation of cutaneous pseudolymphomas and malignant non-Hodgkin lymphomas (36, 37).

To the best of our knowledge this study demonstrates for the first time the full benefit of DNA measurements for the diagnosis of MM on imprint specimens using a computerized high-resolution IA system. Statistical evaluation was performed using 12 features in a stepwise multivariate discriminant analysis. A diagnostic sensitivity of 89.7% and a specificity of 88.9% was attained using a combination of three features: Standard deviation of nuclear area (SAREA), mean nuclear DNA content (MDNA), and 95th percentile of DNA histogram (PERC95).

Material and Methods

Patients

DNA measurements were performed on imprint preparations of skin lesions from 63 patients with melanocytic lesions. The diagnosis was established from histological sections by two independent dermatopathologists. DNA analysis was performed without knowledge of histpathologic diagnosis. Of the 63 cases, 18 were classified as MN (2 of junctional type, 10 of compound type, 5 of dermal type, 1 combined nevus), 6 as dysplastic melanocytic nevi (DN) according to the criteria given by Clark (38), 19 as superficial spreading MM (SSM) and 14 as nodular MM (NMM). One MM could not be further classified. In addition, five metastases of MM were analyzed. Of the melanomas studied 11.8% were of Clark level II, 44.1% of level III, 41.2% of level IV and 2.9% of level V. Tumor thickness was below 0.75 mm in 32.3%, between 0.76 and 1.5 mm in 32.3% and higher than 3.0 in 8.8% of the cases studied. Mitotic rate per mm^2 was equal to or below 1.0/mm2 in 11.8% of the melanomas, between 1.01 and 5.0 /mm2 in 58.8%, and

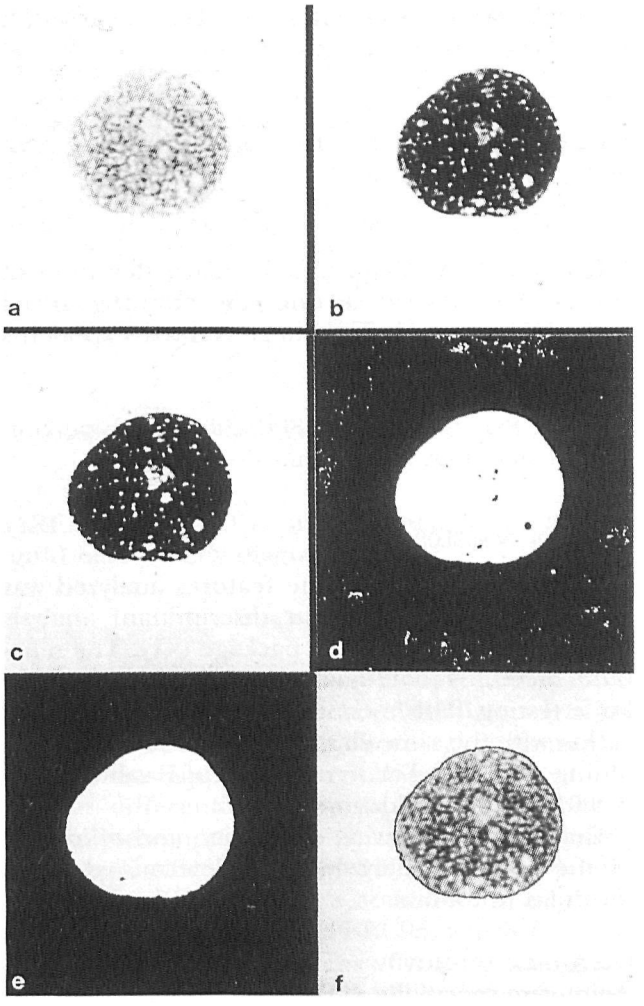

Fig. 1. Steps for automatic detection of nuclear border of a melanocytic cell.
a: original video image. b: mapping of the actual grey levels linearly into the full range of grey values. c: application of the function EMPHASE, which performs an addition of the original image with the difference of the original image and the low-passed filtered version of it. d: detection of the contour of the nucleus using a grey value threshold of 130 in image c. e: smoothing of the contour by applying a dilatation and erosion subsequently. By this step small holes within the object are filled. f: interactive control of segmentation.

higher than 5.0 /mm2 in 29.4% of the tumors. For detailed data concerning patients, age, and sex, see Table 1.

Imprints

Imprints were prepared on clean glass slides by applying the freshly cut surface of a skin biopsy. The imprints were fixed in methanol (100%), formaldehyde (37%), and glacial acetic acid (96%) 85:10:5 (V/V/V). Feulgen-staining was performed according to Böhm (39) with hydrolysis in 5n HCL for 50 min at 28°C and staining in Schiffs reagent for 60 min.

DNA measurements

DNA analysis was performed by the high-resolution image analysis system IPS (Kontron, Eching, Germany). The imprint specimens were digitalized with a density of 16 pixels/μm using a TV Pasecon camera (Bosch, Stuttgart, Germany) connected with a 100-oil objective of an Axioplan microscope (Zeiss, Oberkochen, Germany).

Automatic segmentation

In a first step, the contrast within the original video image (see Fig. 1a) was increased by mapping the actual grey levels linearly into the full range between black (grey value 0) and white (grey value 255) (see Fig. 1b). The contour of the nuclei was automatically found using the function EMPHASE, which reproduced an addition of the original image with the difference of the original image and the low-passed filtered version of it (Fig. 1c). Subsequently, a constant grey value threshold of 130 was used for the automatic segmentation of the nuclei (Fig. 1d). By applying a dilatation and erosion, the outer contour of the nuclei was smoothed out (Fig. 1e). In the same step the holes inside were filled. Inaccurate segmentation could be rejected interactively, because the contour was given in the overlay of the original image at the end of the segmentation process (Fig. 1f).

Parameters calculated

For each nucleus the optical density (OD) and the area were calculated. The integrated optical density (IOD) was obtained as the product of the OD and the area. In Feulgen-stained nuclei the IOD is linearly correlated with the DNA content (39). In each slide 20 chicken erythrocytes were used as an internal reference. In a previous pilot study a comparison of chicken erythrocytes and normal human lymphocytes revealed the following relationship: $OD_{cry} \times 3.26 = 2cDNA$. 2c is the normal DNA content of a human cell. A euploid cell in G2-phase contains 4cDNA. In this study, the relative DNA content in each of 100 randomly selected cells was calculated as follows: relative DNA content = IOD nucleus/IOD1cDNA.

Simultaneous analyses of some imprints stained with May-Grünwald staining, which allows a clear differentiation between melanocytic cells and keratinocytes due to both cellular and nuclear features, proved that most of the cells on imprints were of melanocytic origin. However, a morphologic differentiation of melanocytic cells from other cells (e.g. keratinocytes) cannot be definitely performed in Feulgen stained imprints.

Table 2. Univariate classification of melanocytic nevi and malignant melanomas

Variables	Melanocytic Nevi		Malignant Melanomas		F values
	Mean	SD	Mean	SD	
SAREA	16.49	4.03	28.85	7.55	42.37*
MAREA	76.33	8.89	107.44	26.95	22.64*
MDNA	2.07	0.68	2.90	1.40	5.67
SDNA	0.11	0.14	0.28	0.29	5.69
M2cDI	0.10	0.09	2.53	2.16	14.55
S2cDI	0.49	0.43	2.58	2.35	13.97
M2cDIM	0.59	1.52	3.04	4.14	5.92
S2cDIM	0.16	0.39	1.23	1.84	5.92
5cER	0.06	0.24	2.85	5.05	5.44
PERC80	2.11	0.18	3.18	1.22	31.70*
PERC90	2.16	0.08	3.49	1.13	24.67*
PERC95	2.25	0.06	3.89	1.04	18.78*

For explanation of variables, see Material and Methods. Significant F-values for $p < 0.0001$ are marked by an asterisk.

Special DNA algorithms for data evaluation

The discriminating power of the following features of the DNA histogram was also evaluated:

Mean 2c deviation index (M2cDI)

The 2cDI is defined according to Böcking et al. (40) as the ratio between the sum of the squares of the differences between the DNA values of individual cells (c_i) and the 2c value and the number of cells measured (N):

$$2cDI = \frac{1}{N}\sum_{i=1}^{N}(c_i - 2c)^2$$

Roughly, the 2cDI reflects the variation of the nuclear DNA around the 2c value within one case. The standard deviation of the 2cDI was also calculated (S2cDI). In addition, the modified mean and standard deviation of the 2cDI (M2cDIM, S2cDIM) were computed omitting all nuclei with DNA values being integer-valued exponents of 2c ±12.5%. Thus euploid-polyploid cells are not taken into account. A value of 12.5% was considered as the maximum error of measurement (40).

5c exceeding rate (5cER)

The 5cER is defined according to Böcking et al. (40) as the percentage of cells with a DNA content equal or more than 5c. Since euploid-polyploid cells should not contribute to the 5cER, cells with DNA values which are integer valued exponents of 2c ± 12.5% are not taken into account. Thus the 5cER measures only clearly aneuploid cells.

MAREA: Mean value of the nuclear area within one case.

SAREA: Standard deviation of the nuclear area within one case.

MDNA/ SDNA: Mean and standard deviation of the DNA values within one case omitting nuclei with DNA values being integer-valued exponents of 2c ± 12.5% .

Perc 80, Perc 90, Perc 95: 80th/90th/95th percentiles of the DNA histogram.

Statistical evaluation

Statistical evaluation of the features analyzed was performed with the linear discriminant analysis program 7M of the BMDP package (41). The reliability of multivariate analysis was assessed by jackknife testing. This technique performs a reclassification with the same classification matrix, but withholding one case. For significance of F values a $p < 0.0001$ was required.

Diagnostic sensitivity, specificity, and efficiency of the features analyzed were determined using formulas as follows:

Diagnostic sensitivity = TP/(TP + FN) × 100;
diagnostic specificity = TN/(TN + FP) × 100;
diagnostic efficiency = (TN + TP)/(TN + TP + FN + FP) × 100;

whereby TP = true positive, TN = true negative, FP = false positive, FN = false negative results for malignancy.

The reproducibility of DNA measurements was tested by demonstration of the different ploidy peaks in rat liver imprints.

Results

Univariate analysis

Twelve different morphometric and DNA cytometric features were examined in each of the 63 cases. As shown in Table 2, which is based on 68 400 individual measurements in MN and MM, nuclei of MN had lower values than nuclei of MM for all criteria. Univariate analysis revealed significant differences between MN and MM in 5 of 12 criteria (for $p \leq 0.0001$ an F-value higher than 15 is required, see Table 2). The features which discriminated between MN and MM most reliably were (in order of decreasing F-values): SAREA, PERC80, PERC90, MAREA, PERC95, M2cDI, S2cDI. Using

Table 3. Stepwise multivariate analysis: Selected features and their F-values for discrimination of benign and malignant melanocytic lesions at the end of multivariate analysis

Selected variables	F-values	Other variables	F-values
SAREA	12.8	MAREA	0.0
MDNA	3.4	M2CDI	0.1
Perc 95	7.4	S2CDI	0.1
		SDNA	2.1
		Perc80	0.9
		Perc90	0.6
		5CER	0.1
		M2CDIM	0.0
		S2CDIM	0.3

For explanation of variables see materials and methods.

SAREA alone 82.5% of the melanocytic lesions could be correctly diagnosed.

Multivariate analysis

Many of the variables shown in Table 2 measure similar characteristics and therefore they might be correlated. To analyze possible correlations and to find the most appropriate combination of features for the differential diagnosis between MN and MM, stepwise multivariate analysis was performed. Correct classification of 89.5% of the cases analyzed was achieved using a combination of three features: SAREA, MDNA, PERC95, which were included in the first three steps of multivariate analysis (see Table 3 and Fig. 2). The corresponding sensitivities and specificities were 89.7% and 88.9%, respectively. Due to the correlation between some of the features, some variables presenting with high F-values in univariate analysis were less helpful in multivariate analysis, as indicated by

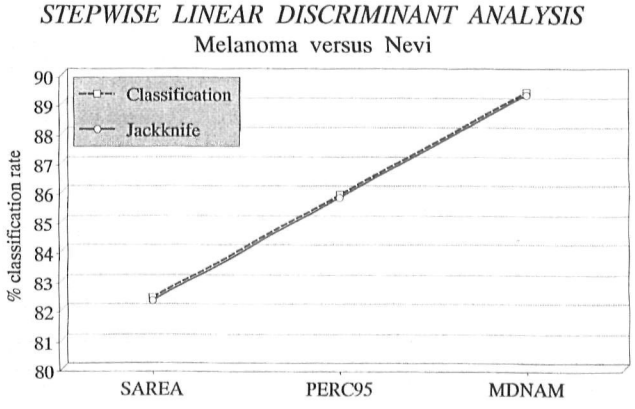

Fig. 2. Stepwise linear discriminant analysis for differentiation between malignant melanoma and melanocytic nevi. Using the three features – standard deviation of nuclear area (SAREA), mean DNA value (MDNA), and 95th percentile of DNA distribution (PERC95) – 89.5% of the MM and MN cases could be correctly diagnosed.

Table 4. Coefficients for calculation of the canonical variable

Selected Variables	Coefficients
SAREA	–0.08918
MDNA	0.55689
PERC95	–1.58452

For explanation of variables see materials and methods.

their low F-values in Table 3 (MAREA, PERC80, PERC90). In contrast, MDNA was included in multivariate analysis although presenting a low F-value in univariate analysis. Classification rate in multivariate analysis was 7% higher than in univariate analysis.

At the end of multivariate analysis the three features selected can be summarized with a linear equation to a new variable termed canonical variable (CANVAR). The coefficients for this equation, given in Table 4, were determined in the BMDP7M program (41). According to its definition, the

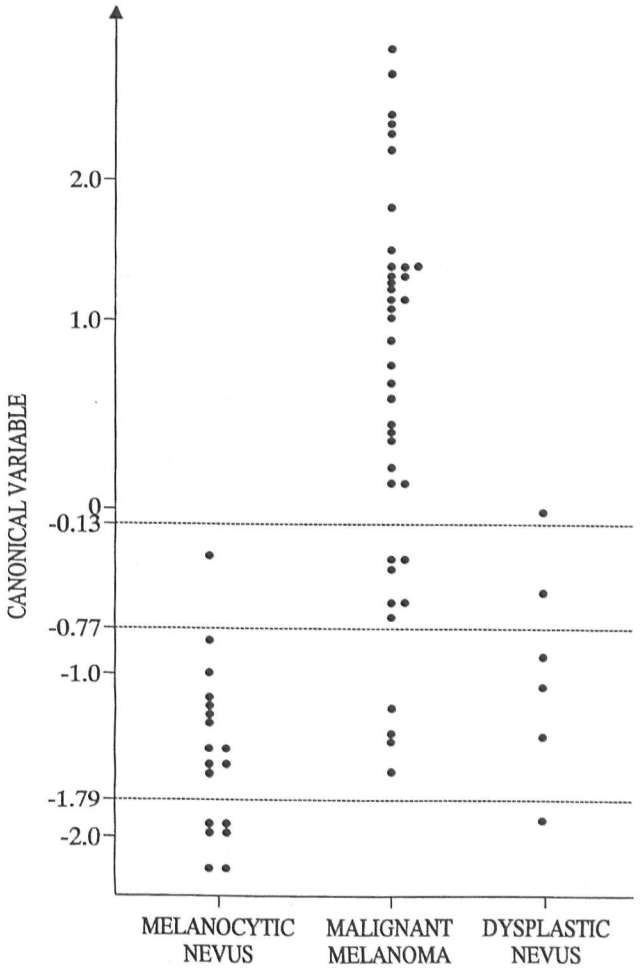

Fig. 3. Using a threshold for the CANVAR of –0.77, 91.2% of the MM and MN could be differentiated. Four of the DN were found in the benign range, whereas 2 were located within the malignant lesions.

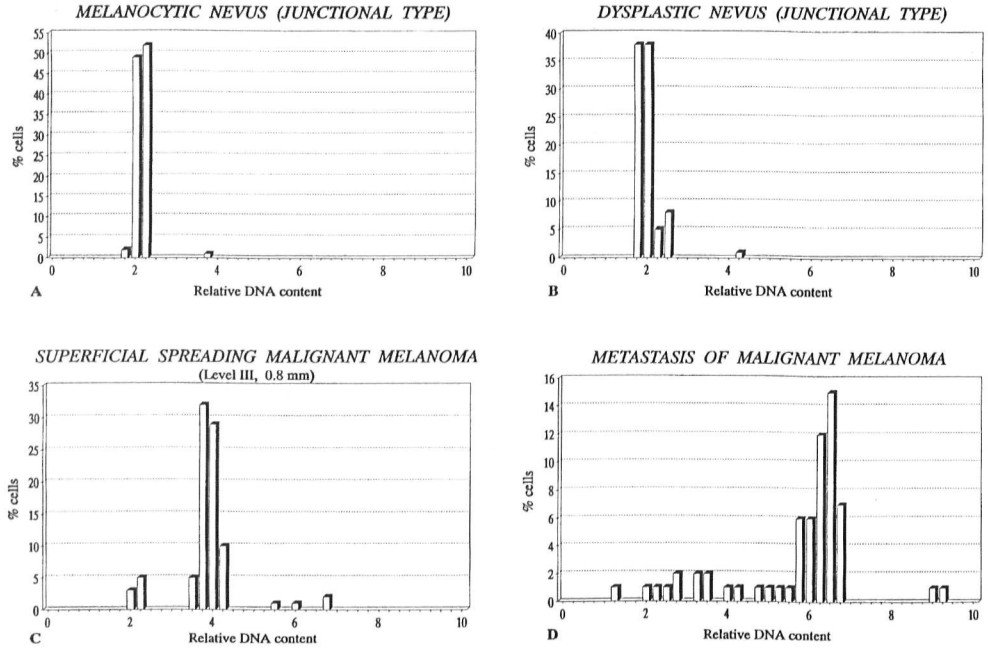

Fig. 4. Four typical patterns of DNA histograms could be found in this study:
a: Example for type I, displaying a distribution with one high peak at 2c and a small peak at 4c with less than 5% of the nuclei with DNA values between 3.5c and 4.5c DNA (type I). Type I was found in 83.3% of the MN. Type II showing bimodal distribution with a high peak (more than 10% of the nuclei) at 4c in addition to the 2c peak. Type II was calculated in 3 cases of MM (not shown in this figure).
b: Type III presents with a bimodal distribution similar to type II, but with more than 5% of the nuclei in the gap between 2.25c and 3.5c (S-phase cells and aneuploid cells). Type III was found most frequently in DN (83.3%) and MM (32.3%).
c, d: Type IV is characterized by at least 1% of the cells with aneuploid DNA values > 5c . Type IV could be observed in 35% of the MM (12 cases) and 100% of the MM metastases. In contrast, only 1 of 18 MN (5%) showed this DNA distribution pattern.

CANVAR has the same discriminant power as the three selected features together. Using the coefficients for calculation of the CANVAR, for each case a new individual canonical value can be calculated from the values of SAREA, MDNA, and PERC95. The higher this CANVAR value, the higher is the chance of malignancy. In our study the CANVAR for MN ranged from −2.20 to −0.35 (mean value −1.52), for primary MM from −1.65 to 2.30 (mean value 0.55). DN displayed CANVAR between −1.99 and 0.0 (mean value −1.04), metastases of MM between 0.38 and 2.73 (mean value 1.63).

Using a threshold provided by multivariate analysis 51 out of 57 cases (89.5%) could be correctly differentiated (see Fig. 3). By applying −0.77 as threshold one could argue that even 52 out of 57 cases (91.2%) could be separated. However, this was not confirmed by statistical analysis, since the difference between the benign and malignant cases at this threshold was too small for a safe distinction. In Fig. 3, CANVAR values above −0.77 were found almost exclusively in MM and all cases of MN were below −0.13. Therefore, in our scale a CANVAR higher than −0.13 can be considered as proof of malignancy. No MM displayed a CANVAR below −1.79.

DNA histograms

The four classical types of DNA histograms (36) could also be found in imprints of melanocytic lesions (see Fig. 4a–d). Fig. 4a depicts a distribution with one high peak at 2c and a small peak at 4c with less than 5% of the nuclei with DNA values between 3.5c and 4.5c DNA (type I). This type was most frequently found in benign MN: 83.3% (15 cases) of MN, but also 23.5% (8 cases) of MM showed this pattern.

Type II (not shown here) depicts a bimodal distribution with a high peak (more than 10% of the nuclei) at 4c in addition to the 2c peak. It was seen in 3 cases of MM.

A bimodal distribution similar to type II, but with more than 5% of the nuclei in the gap between 2.25c and 3.5c (S-phase cells and aneuploid cells) is typical for type III. It was found in 2 of 18 MN (11%), 5 of 6 (83.3%) DN, and in 11 of 34 MM (32.3%) (see Fig. 4b).

The type IV histogram (see Fig. 4c, d), characterized by the presence of at least 1% aneuploid cells having DNA values >5c, could be observed in 35% of the MM (12 cases) and 100% of the MM meta-

stases. In contrast, only 1 of 18 MN (5%) showed this DNA distribution pattern.

Classification of dysplastic nevi (DN)

Fig. 3 shows the classification of DN using the CANVAR values calculated for discrimination between MM and MN. In one case with 0.0 the CANVAR value was clearly in the range of MM. In an additional case, a CANVAR value of –0.61 was found, which is slightly higher than –0.77, the threshold for the separation between MM and MN. Three cases displayed CANVAR values in a zone in which most of the cases were benign and only a few were malignant. One case had a CANVAR value within a zone with MN only.

Discussion

The most important result of this cytometric study was that melanocytic nevi (MN) and malignant melanomas (MM) could be differentiated on imprints with an efficiency of 89.5% using three features, the standard deviation of nuclear area (SAREA), the mean value of DNA content of the nuclei (MDNA), and the 95th percentile of DNA distribution (PERC95). The sensitivity and specificity attained were 89.7% and 88.9%, respectively. The diagnostic efficiency of 89.5% in this study is higher than in 4 out of 6 previous DNA cytometric investigations on sections, in which between 76.1% and about 100% of the cases (mean value 87.5%) were correctly classified (16, 29, 32, 33, 34, 35). The different classification rates in those studies can be explained by different methods of feature extraction, data analysis, definition of aneuploidy, number of cases of each category analyzed, selection of tumors for analysis, and cell sampling strategies. To our knowledge, using FC, only Chi et al. (36) found aneuploidy in all of 20 MM and could therefore clearly distinguish them from benign nevi and Spitz nevi. However, all of their probes were taken from advanced nodular lesions being unequivocal for histopathologists.

It is impressive that the efficiency of discrimination between MM and MN in imprint specimens using IA is equal to or even higher than in studies using sections for DNA measurements with IA (29, 32, 35) or CP (33). It can be speculated that on imprint specimens DNA features are especially helpful, because the whole nucleus can always be definitely measured, which is not possible on sections. Since IA of imprints of melanocytic lesions reveal results at least of the same efficiency as of sections, imprints can be recommended for future investigations for two reasons: a) A rapid preparation after excision without loss of potentially important tissue is possible. b) Time-saving automatic detection of the borders with fully automatic feature-analysis can be performed. Therefore the measurement of 100 melanocytic nuclei can be done in less than 30 min. Nevertheless, also archival material can be analyzed, since imprints can also be obtained from paraffin blocks, although the probability of detecting aneuploid nuclei is more likely on imprints of fresh than of paraffin-embedded tissue (42). The interesting results obtained here on imprints of MM and MN by IA were in agreement with those of a cytophotometric study of Bergman (16). He could also differentiate between MM and MN in 89.7% of the cases. However, CP is much more time-consuming than IA and morphometric features cannot be determined simultaneously (23, 24).

A drawback to the analysis of Feulgen-stained imprint specimens is, that it is not definitely possible to discriminate tumor cells from other not interesting cells, e.g. keratinocytes. However, analyses of May-Grünwald stained imprints of melanocytic lesions disclosed that keratinocytes were not abundant, since the adherence of non-tumor cells in the tissue is much higher than of melanocytic cells. Moreover, if keratinocytes are also measured, these diploid cells do not cause false positive results.

The tendency towards higher proliferation and appearance of polyploid and aneuploid cells in malignant melanocytic tumors is documented by the finding of four different types of DNA histograms in our study (Fig. 4). The results obtained from the currently controversially discussed group of DN (43–46) also indicate an increased proliferation of melanocytes within this group. However, true aneuploidy was not detected in DN, which is in agreement with the data of a recent cytometric study of 38 cases fulfilling the histologic criteria of DN (47). Five of 6 lesions presented a type III histogram, displaying a bimodal distribution with more than 5% of the nuclei in the space between 2.25c and 3.5c, probably S-phase cells. In addition, also the CANVAR values of DN supported the intermediate position of dysplastic nevi in the transition zone between benign and malignant, as already speculated (16, 31, 35, 30). However DN could not be separated from MM and MN by morphometric and cytometric criteria as a distinct entity.

Thousands of cells can also be analyzed within minutes by FC (22), which was frequently used for DNA measurements of melanocytic lesions (25–30). However, in FC, the interpretation of hypertetraploid signals of low frequency is difficult due to the high rate of false alarms caused by aggregated cells (48). Autofluorescence of melanocytic

nuclei and destroyed cells might also contribute to bias and explains the limited diagnostic efficiency of FC compared to IA. IA permits visual examination of each cell and interactive rejection of clumped and destroyed nuclei is possible. Thus, diagnostically important cells with high DNA values strongly influencing the value for the 95th percentile and mean DNA value can be detected with high accuracy (24). In MM, FC seems to be more useful for prognostic evaluation (49, 50).

Differentiation between MM and MN was also performed in light microscopy applying pure morphometric and stereologic analyses (5, 6, 51). The importance of morphometric data for the discrimination between MM and MN can also be seen in this study, because of the classification rate of 82.5% for SAREA, which was the best criterion in univariate analysis. However, classification rates could be increased to 89.5%, if DNA cytometric features were included.

IA, the most general approach to cell analysis, is an adequate method for extracting a multitude of features with high accuracy (24). Moreover, IA allows also the evaluation of a variety of chromatin features, e.g. the amount of eu- and heterochromatin, chromatin homogeneity, and chromatin aggregations (21, 24). In a recent ultrastructural study applying 34 different morphometric and chromatin features, all of the cases could be correctly classified as MN or MM due to the characterization of markedly atypical cells (MACS) (52). MACS were selected by eight different features describing the amount of eu- and heterochromatin, chromatin aggregations and nuclear morphology. Therefore it seems to be possible that the diagnostic efficiency can be further improved by chromatin texture analysis, as was also recently demonstrated in a multiparametric study of Fleming and Friedman (53) . Also the developments in artificial intelligence involving neural networks may facilitate the diagnostic process in the future (54).

Acknowledgment

The skillful technical assistance of Mrs. E. Januschke and Mrs. I. Pfab is gratefully acknowledged.

References

1. Jones RE. What are your five most important histological criteria for the diagnosis of malignant melanoma? Am J Dermatopathol 1984: 6: 337.
2. Schmoeckel C. How consistent are dermatopathologists in reading early malignant melanoma and lesions precursor to them? An international survey. Am J Dermatopathol 1983: 6 (suppl 1): 13.
3. Tron VA, Barnhill RL, Mihm MC. Malignant melanoma in situ: Functional considerations of cancer. Human Pathol 1990: 21: 1202.
4. Larsen TE, Little JH, Orell SR, Prade M. International pathologists congruence survey on quantitation of malignant melanoma. Pathology 1980: 12: 245.
5. Leitinger G, Cerroni L, Soyer HP, Smolle J, Kerl H. Morphometric diagnosis of melanocytic skin tumors. Am J Dermatopathol 1990: 12: 441.
6. Stolz W, Schmoeckel C, Ryckmanns F, Groß J, Braun-Falco O. Morphometric and ultrastructural analyses of melanocytes, nevus cells, and melanoma cells. Arch Dermatol Res 1987: 279: 167.
7. Lindholm C, Hofer PA. Caryometry of benign compound acquired naevi, Spitz epitheloid naevi, and malignant melanomas. Acta Pathol Microbiol Immunol Scand (A) 1986: 94: 371.
8. Herlyn M, Clark WH, Rodeck U, Mancianti ML, Jambrosic J, Koprowski H. Biology of disease: Biology of tumor progression in human melanocytes. Lab Invest 1987: 56: 461.
9. Johnson JP, Stade BG, Rothbächer U, Lehmann JM, Riethmüller G. Melanoma antigens and their association with malignant transformation and tumor progression. In: Ferrone S, ed. Malignant melanoma. Berlin, Heidelberg, New York: Springer, 1990: 106.
10. Ruiter DJ. Melanomas and other skin neoplasms. Pathology and case reports. Curr Opin Oncol 1990: 2: 377.
11. Herlyn M, Thurin J, Balaban G. Characteristics of cultured human melanocytes, isolated from different stages of tumor progression. Cancer Res 1985: 45: 5670.
12. Balaban GB, Herlyn M, Clark WH. Karyotypic evolution in human malignant melanoma. Cancer Genet Cytogenet 1986: 19: 113.
13. Trent JM. Cytogenetics of human malignant melanoma. In: Balch CM, Houghton AN, eds. Cutaneous melanoma. 2nd edition. Philadelphia, Lippincott, 1992: 101.
14. Grammatico P, LoRe ML, Scarpa S, Modesti A, Del Porto G. Human malignant melanoma. Significance of chromosomal abnormalities. Cancer Genet Cytogenet 1990: 48: 237.
15. Hall TJ, Fu YS. Applications of quantitative microscopy in tumor pathology. Lab Invest 1985: 53: 5.
16. Bergman W, Ruiter DJ, Scheffer D, van Vloten WA. Melanocytic atypia in dysplastic nevi. Immunohistochemical and cytophotometric analysis. Cancer 1988: 61: 1660.
17. Schmiegelow P, Schroiff R, Breitbart E, Bahnsen J, Lindner J, Jänner M. Malignant melanoma – its precursors and its topography of proliferation. DNA-Feulgen-cytophotometry and mitosis index. Virchows Arch A (Pathol Anat) 1986: 409: 47.
18. Zardawi IM, Jarvis LR, Francis L, Shaw HM, Grace J. DNA ploidy in thin melanoma. Pathology 1988: 20: 243.
19. Barlogie B, Drewinko B, Schumann J, et al. Cellular DNA content as a marker of neoplasia in man. Am J Med 1980: 69: 195.
20. Büchner T, Hiddemann W, Wörmann B, Kleinemeier B. Differential pattern of DNA-aneuploidy in human malignancies. Pathol Res Pract 1985: 179: 310.
21. Stolz W, Vogt Th, Landthaler M, Abmayr W. Computerized quantitative dermatopathology. In: Stoecker W, ed. Computer applications in dermatology. New-York: Igaku-Shoin, 1993: 117.

22. Koss LG, Czerniak B, Herz F, Wersto RP. Flow cytometric measurements of DNA and other cell components in human tumors: A critical apprisal. Human Pathol 1989: 20: 528.
23. Auer G, Askensten U, Ahrens O. Cytophotometry. Human Pathol 1989: 20: 518.
24. Wied GL, Bartels PH, Bibbo M, Dytch HE. Image analysis in quantitative cyto- and histopathology. Human Pathol 1989: 20: 549.
25. Søndergaard K, Larsen JK, Møller U, Christensen IJ, Hou-Jensen K. DNA ploidy characteristics of human malignant melanoma analysed by flow cytometry and compared with histology and clinical course. Vichows Arch B (Cell Pathol) 1983: 42: 53.
26. Von Roenn JH, Kheir SM, Wolter JM, Coon JS. Significance of DNA abnormalities in primary malignant melanoma and nevi: a retrospective flow cytometric study. Cancer Res 1986: 46: 3192.
27. Kamino H, Ratech H. Improved detection of aneuploidy in malignant melanoma using multiparameter flow-cytometry for S100 protein and DNA content. J Invest Dermatol 1989: 93: 392.
28. Chi HI, Ishibashi Y, Shima A, Mihara I, Otsuka F. Use of DAPI cytofluorometric analysis of cellular DNA content to differentiate Spitz nevus from malignant melanoma. J Invest Dermatol 1990: 95: 154.
29. Sangueza OP, Hyder DM, White CR, et al. Comparison of image analysis with flow cytometry for DNA content analysis in pigmented lesions of the skin. Anal Quant Cytol Histol 1992: 14: 55.
30. Slater SD, Cook MG, Fisher C, Wright NAW, Foster CS. A comparative study of proliferation indices and ploidy in dysplastic naevi and malignant melanomas using flow cytometry. Histopathol 1991: 19: 337.
31. Newton JA, Camplejohn RS, McGibbon DH. The flow cytometry of melanocytic skin lesions. J Invest Dermatol 1988: 91: 380.
32. LeBoit PE, Fletcher HV. A comparative study of Spitz nevus and nodular malignant melanoma using image analysis cytometry. J Invest Dermatol 1987: 88: 753.
33. Lindholm C, Bjelkenkrantz K, Hofer P. DNA-cytophotometry of benign compound and intradermal naevi, Spitz epitheloid naevi and malignant melanomas. Virchows Arch B: 1987: 257.
34. Rode J, Williams RA, Jarvis LR, Dhillon AP, Jamal O. S100 Protein, neurone specific enolase, and nuclear DNA content in Spitz naevus. J Pathol 1990: 161: 41.
35. Fleming MG, Wied GL, Dytch HE. Image analysis cytometry of dysplastic nevi. J Invest Dermatol 1990: 95: 287.
36. Stolz W, Vogt T, Braun Falco O, et al. Differentiation between lymphomas and pseudolymphomas of the skin by computerized DNA-image cytometry. J Invest Dermatol 1990: 94: 254.
37. Vogt T, Stolz W, Braun-Falco O, et al. Prognostic significance of DNA cytometry in cutaneous malignant lymphomas. Cancer 1991: 68: 1095.
38. Clark WH, Elder DE, Guerry D, Epstein MN, Greene MH, van Horn MM. The precursor lesion of superficial spreading and nodular melanoma. Hum Pathol 1984: 15: 1145.
39. Böhm N. Einfluß der Fixierung und der Säurekonzentration auf die Feulgen Hydrolyse bei 28° C. Histochemie 1968: 14: 201.
40. Böcking A, Adler C-P, Common HH, Hilgarth M, Granzen B, Auffermann W. Algorithm for a DNA-cytophotometric diagnosis and grading of malignancy. Anal Quant Cytol 1984: 6: 1.
41. Dixon WJ. BMDP statistical software. Berkeley, University of California press, 1981.
42. Herzberg AJ, Kerns BJ, Borowitz MJ, Seigler HF, Kinney RB. DNA ploidy of malignant melanoma determined by image cytometry of fresh frozen and paraffin-embedded tissue. J Cutan Pathol 1991: 18: 440.
43. Ackerman AB, Mihara I. Dysplasia, dysplastic melanocytes, dysplastic nevi, the dysplastic nevus syndrome, and the relation between dysplastic nevi and malignant melanoma. Hum Pathol 1985: 16: 87.
44. Ackerman AB. What nevus is dysplastic, a syndrome and the commonest precursor of malignant melanoma? A riddle and an answer. Histopathol 1988 : 13: 241.
45. Jones RE. Do you make the histologic diagnosis of dysplastic nevus? Am J Dermatopathol 1987: 7: 213.
46. Rywlin AM. Malignant melanoma in the light of the multistep theory of neoplasia. Am J Dermatopathol 1989: 11: 387.
47. Sangueza OP, Hyder DM, Bakke AC, White CR. DNA determination in dysplastic nevi. A comparative study between flow cytometry and image analysis. Am J Dermatopathol 1993: 15: 99.
48. Ploem-Zaajer JJ, van Driel-Kulker AM, Mesker WE, Cornelisse CJ. Advantages and limitations of retrospective DNA cytometry by flow and image analysis. In: Burger G, Ploem JS, Goerttler K, eds. Clinical Cytometry and Histometry. London, San Diego, New York: Academic Press, 1987: 176.
49. Bines SD, von Roenn JH, Kheir SM, Coon JS. Flow Cytometry in Melanoma. In: Nathanson L, ed. Malignant Melanoma: Biology, Diagnosis, and Therapy. Boston: Kluwer Academic Publishers, 1988: 172.
50. Bartkowiak D, Otto F, Schuman J, Lippold A, Drepper H. Sequential DNA flow cytometry in metastatic malignant melanoma. Oncology 1991: 48: 154.
51. Olinici CD, Giurgiuman M. Morphometric studies on melanocytic tumors. Morphol Embryol 1989: 35: 49.
52. Stolz W, Abmayr W, Schmoeckel C, Landthaler M, Massoudy P, Braun-Falco O. Ultrastructural discrimination between malignant melanomas and benign nevocytic nevi using high-resolution image and multivariate analysis. J Invest Dermatol 1991: 97: 903.
53. Fleming MG, Friedman RJ. Multiparametric image cytometry of nevi and melanomas. Am J Dermatopathol 1993: 15: 106.
54. Baak JP. Artificial intelligence systems (expert sytems) as diagnostic consultants for the cytologic and histologic diagnosis of cancer. J Cancer Res Clin Oncol 1988: 114: 325.
55. Bingler P. DNA-Zytometrie melanozytärer Hautveränderungen. Munich, Germany: LM-University of Munich, 1993. 112 pp. Dissertation.